A Hybrid High-Order method for the incompressible Navier–Stokes problem based on Temam's device

L. Botti   D. A. Di Pietro   J. Droniou

Institut Montpelliérain Alexander Grothendieck, University of Montpellier

EDF, 28 June 2018

HHO: The inner circle

- Joubine Aghili (Université de Nice)
- Sébastien Boyaval (École des Ponts ParisTech)
- Daniele Boffi (Università di Pavia)
- Francesco Bonaldi (Politecnico di Milano)
- Lorenzo Botti (Università di Bergamo)
- Michele Botti (Université de Montpellier)
- Florent Chave (Université de Montpellier and Politecnico di Milano)
- Bernardo Cockburn (University of Minnesota)
- Jérôme Droniou (Monash University)
- Alexandre Ern (École des Ponts ParisTech)
- Luca Formaggia (Politecnico di Milano)
- Giuseppe Geymonat (École Polytechnique)
- Françoise Krasucki (Université de Montpellier)
- Stella Krell (Université de Nice)
- Simon Lemaire (INRIA)
- Alexander Linke (Weierstraß Institute Berlin)
- Gianmarco Manzini (Los Alamos National Laboratories)
- Fabien Marche (Université de Montpellier)
- Franck Pigeonneau (Saint-Gobain Recherche)
- Berardo Ruffini (Université de Montpellier)
- Friedhelm Schieweck (Otto-von-Güricke Universität)
- Pierre Sochala (BRGM)
- Ruben Specogna (Università di Udine)
- . . .

Features

- Capability of handling general polyhedral meshes
- Construction valid for arbitrary space dimensions
- Arbitrary approximation order (including $k = 0$)
- Robustness with respect to the variations of the physical coefficients
- Local conservation of relevant physical quantities
- Reduced computational cost after static condensation

Outline

Outline

Key ideas

- Discrete unknowns at elements and faces
- Local reconstructions inspired from local projectors
- No explicit expression for the basis functions
- High-order stabilisation inside each element
- Fully discrete formulation [DP and Droniou, 2018]

Polyhedral meshes

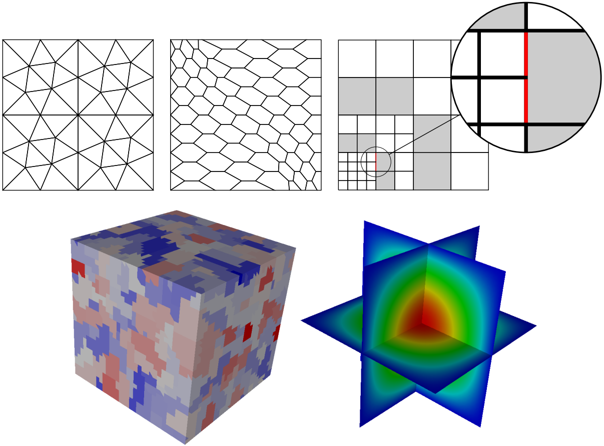

Figure: Supported meshes in 2d and 3d, and HHO solution on the agglomerated 3d mesh. For the notions of polytopal mesh and regular polytopal mesh sequence see [DP and Tittarelli, 2018]

Model problem

- Let $\Omega \subset \mathbb{R}^d$, $d \geq 1$, denote a bounded, connected polyhedral domain
- For $f \in L^2(\Omega)$, we consider the Poisson problem

$$\begin{aligned} -\Delta u &= f && \text{in } \Omega \\ u &= 0 && \text{on } \partial\Omega \end{aligned}$$

- In weak form: Find $u \in H_0^1(\Omega)$ s.t.

$$a(u,v) := (\nabla u, \nabla v) = (f, v) \qquad \forall v \in H_0^1(\Omega)$$

Projectors on local polynomial spaces

- At the core of HHO are projectors on local polynomial spaces
- With $X = T$ or $X = F$, the L^2-projector $\pi_X^{0,l} : L^1(X) \to \mathbb{P}^l(X)$ is s.t.

$$(\pi_X^{0,l} v - v, w)_X = 0 \text{ for all } w \in \mathbb{P}^l(X)$$

- The elliptic projector $\pi_T^{1,l} : W^{1,1}(T) \to \mathbb{P}^l(T)$ is s.t.

$$(\boldsymbol{\nabla}(\pi_T^{1,l} v - v), \boldsymbol{\nabla} w)_T = 0 \text{ for all } w \in \mathbb{P}^l(T) \text{ and } \int_T (\pi_T^{1,l} v - v) = 0$$

- Both $\pi_T^{0,l}$ and $\pi_T^{1,l}$ have optimal approximation properties in $\mathbb{P}^l(T)$
- See [DP and Droniou, 2017a, DP and Droniou, 2017b]

Computing $\pi_T^{1,k+1}$ from L^2-projections of degree k

- The following integration by parts formula is valid for all $v \in H^1(T)$ and all $w \in C^\infty(\overline{T})$:

$$\boxed{(\nabla v, \nabla w)_T = -(v, \Delta w)_T + \sum_{F \in \mathcal{F}_T} (v, \nabla w \cdot \boldsymbol{n}_{TF})_F}$$

- Specializing it to $w \in \mathbb{P}^{k+1}(T)$, we can write

$$(\nabla \pi_T^{1,k+1} v, \nabla w)_T = -(\pi_T^{0,k} v, \Delta w)_T + \sum_{F \in \mathcal{F}_T} (\pi_F^{0,k} v_{|F}, \nabla w \cdot \boldsymbol{n}_{TF})_F$$

- Moreover, it can be easily seen that

$$\int_T (\pi_T^{1,k+1} v - v) = \int_T (\pi_T^{1,k+1} v - \pi_T^{0,k} v) = 0$$

- **Hence, $\pi_T^{1,k+1} v$ can be computed from $\pi_T^{0,k} v$ and $(\pi_F^{0,k} v_{|F})_{F \in \mathcal{F}_T}$!**

Discrete unknowns

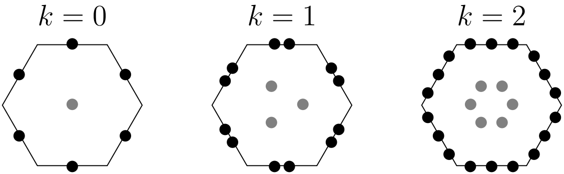

Figure: $\underline{U}_T^k$ for $k \in \{0, 1, 2\}$

- Let a polynomial degree $k \geq 0$ be fixed
- For all $T \in \mathcal{T}_h$, we define the local space of discrete unknowns

$$\underline{U}_T^k := \left\{ \underline{v}_T = (v_T, (v_F)_{F \in \mathcal{F}_T}) \ : \ v_T \in \mathbb{P}^k(T) \text{ and } v_F \in \mathbb{P}^k(F) \quad \forall F \in \mathcal{F}_T \right\}$$

- The local interpolator $\underline{I}_T^k : H^1(T) \to \underline{U}_T^k$ is s.t., for all $v \in H^1(T)$,

$$\underline{I}_T^k v := (\pi_T^{0,k} v, (\pi_F^{0,k} v_{|F})_{F \in \mathcal{F}_T})$$

Local potential reconstruction

- Let $T \in \mathcal{T}_h$. We define the local potential reconstruction operator

$$r_T^{k+1} : \underline{U}_T^k \to \mathbb{P}^{k+1}(T)$$

s.t. for all $\underline{v}_T \in \underline{U}_T^k$, $\int_T (r_T^{k+1}\underline{v}_T - v_T) = 0$ and

$$\boxed{(\nabla r_T^{k+1}\underline{v}_T, \nabla w)_T = -(v_T, \Delta w)_T + \sum_{F \in \mathcal{F}_T} (v_F, \nabla w \cdot \boldsymbol{n}_{TF})_F \quad \forall w \in \mathbb{P}^{k+1}(T)}$$

- By construction, we have

$$\boxed{r_T^{k+1} \circ \underline{I}_T^k = \pi_T^{1,k+1}}$$

- $r_T^{k+1} \circ \underline{I}_T^k$ has therefore optimal approximation properties in $\mathbb{P}^{k+1}(T)$

Stabilization I

- We would be tempted to approximate

$$a_{|T}(u,v) \approx (\boldsymbol{\nabla} r_T^{k+1}\underline{u}_T, \boldsymbol{\nabla} r_T^{k+1}\underline{v}_T)_T$$

- This choice, however, is not stable in general. We consider instead

$$\boxed{\mathrm{a}_T(\underline{u}_T,\underline{v}_T) := (\boldsymbol{\nabla} r_T^{k+1}\underline{u}_T, \boldsymbol{\nabla} r_T^{k+1}\underline{v}_T)_T + \mathrm{s}_T(\underline{u}_T,\underline{v}_T)}$$

- The role of s_T is to ensure $\|\cdot\|_{1,T}$-coercivity with

$$\|\underline{v}_T\|_{1,T}^2 := \|\boldsymbol{\nabla} v_T\|_T^2 + \sum_{F\in\mathcal{F}_T} \frac{1}{h_F}\|v_F - v_T\|_F^2 \quad \forall \underline{v}_T \in \underline{U}_T^k$$

Stabilization II

Assumption (Stabilization bilinear form)

The bilinear form $\mathrm{s}_T : \underline{U}_T^k \times \underline{U}_T^k \to \mathbb{R}$ satisfies the following properties:

- Symmetry and positivity. s_T is symmetric and positive semidefinite.
- Stability. It holds, with hidden constant independent of h and T,

$$\mathrm{a}_T(\underline{v}_T, \underline{v}_T)^{\frac{1}{2}} \simeq \|\underline{v}_T\|_{1,T} \quad \forall \underline{v}_T \in \underline{U}_T^k.$$

- Polynomial consistency. For all $w \in \mathbb{P}^{k+1}(T)$ and all $\underline{v}_T \in \underline{U}_T^k$,

$$\mathrm{s}_T(\underline{I}_T^k w, \underline{v}_T) = 0.$$

Stabilization III

- The following stable choice violates polynomial consistency:

$$\mathrm{s}_T^{\mathrm{hdg}}(\underline{u}_T, \underline{v}_T) \coloneqq \sum_{F \in \mathcal{F}_T} h_F^{-1}(u_F - u_T, v_F - v_T)_F$$

- To circumvent this problem, we penalize the high-order differences

$$(\delta_T^k \underline{v}_T, (\delta_{TF}^k \underline{v}_T)_{F \in \mathcal{F}_T}) \coloneqq \underline{I}_T^k r_T^{k+1} \underline{v}_T - \underline{v}_T$$

- The classical HHO stabilization bilinear form reads

$$\boxed{\mathrm{s}_T(\underline{u}_T, \underline{v}_T) \coloneqq \sum_{F \in \mathcal{F}_T} h_F^{-1}((\delta_T^k - \delta_{TF}^k)\underline{u}_T, (\delta_T^k - \delta_{TF}^k)\underline{v}_T)_F}$$

Discrete problem

- Define the global space with single-valued interface unknowns

$$\underline{U}_h^k := \Big\{ \underline{v}_h = ((v_T)_{T\in\mathcal{T}_h}, (v_F)_{F\in\mathcal{F}_h}) \ : \\ v_T \in \mathbb{P}^k(T) \quad \forall T \in \mathcal{T}_h \text{ and } v_F \in \mathbb{P}^k(F) \quad \forall F \in \mathcal{F}_h \Big\}$$

  and its subspace with strongly enforced boundary conditions

$$\underline{U}_{h,0}^k := \left\{ \underline{v}_h \in \underline{U}_h^k \ : \ v_F = 0 \quad \forall F \in \mathcal{F}_h^{\mathrm{b}} \right\}$$

- The discrete problem reads: Find $\underline{u}_h \in \underline{U}_{h,0}^k$ s.t.

$$\boxed{\mathrm{a}_h(\underline{u}_h, \underline{v}_h) := \sum_{T\in\mathcal{T}_h} \mathrm{a}_T(\underline{u}_T, \underline{v}_T) = \sum_{T\in\mathcal{T}_h} (f, v_T)_T \quad \forall \underline{v}_h \in \underline{U}_{h,0}^k}$$

- Well-posedness follows from coercivity and discrete Poincaré

Convergence

Theorem (Energy-norm error estimate)

Assume $u \in H_0^1(\Omega) \cap H^{k+2}(\mathcal{T}_h)$. The following energy error estimate holds:

$$\boxed{\|\boldsymbol{\nabla}_h(r_h^{k+1}\underline{u}_h - u)\| + |\underline{u}_h|_{s,h} \lesssim h^{k+1}|u|_{H^{k+2}(\mathcal{T}_h)},}$$

with $(r_h^{k+1}\underline{u}_h)_{|T} := r_T^{k+1}\underline{u}_T$ for all $T \in \mathcal{T}_h$ and $|\underline{u}_h|_{s,h}^2 := \sum_{T\in\mathcal{T}_h} \mathrm{s}_T(\underline{u}_T, \underline{u}_T)$.

Theorem (Superclose L^2-norm error estimate)

Further assuming elliptic regularity and $f \in H^1(\mathcal{T}_h)$ if $k = 0$,

$$\boxed{\|r_h^{k+1}\underline{u}_h - u\| \lesssim h^{k+2}\mathcal{N}_k,}$$

with $\mathcal{N}_0 := \|f\|_{H^1(\mathcal{T}_h)}$ and $\mathcal{N}_k := |u|_{H^{k+2}(\mathcal{T}_h)}$ for $k \geq 1$.

Static condensation I

- Fix a basis for $\underline{U}_{h,0}^{k}$ with functions supported by only one T or F
- Partition the discrete unknowns into element- and interface-based:

$$\mathsf{U}_h = \begin{bmatrix} \mathsf{U}_{\mathcal{T}_h} \\ \mathsf{U}_{\mathcal{F}_h^{\mathrm{i}}} \end{bmatrix}$$

- U_h solves the following linear system:

$$\begin{bmatrix} \mathsf{A}_{\mathcal{T}_h\mathcal{T}_h} & \mathsf{A}_{\mathcal{T}_h\mathcal{F}_h^{\mathrm{i}}} \\ \mathsf{A}_{\mathcal{F}_h^{\mathrm{i}}\mathcal{T}_h} & \mathsf{A}_{\mathcal{F}_h^{\mathrm{i}}\mathcal{F}_h^{\mathrm{i}}} \end{bmatrix} \begin{bmatrix} \mathsf{U}_{\mathcal{T}_h} \\ \mathsf{U}_{\mathcal{F}_h^{\mathrm{i}}} \end{bmatrix} = \begin{bmatrix} \mathsf{F}_{\mathcal{T}_h} \\ 0 \end{bmatrix}$$

- $\mathsf{A}_{\mathcal{T}_h\mathcal{T}_h}$ **is block-diagonal and SPD, hence inexpensive to invert**

Static condensation II

This remark suggests a two-step solution strategy:

- Element unknowns are eliminated solving the local balances

$$\mathsf{U}_{\mathcal{T}_h} = \mathsf{A}_{\mathcal{T}_h\mathcal{T}_h}^{-1}\left(\mathsf{F}_{\mathcal{T}_h} - \mathsf{A}_{\mathcal{T}_h\mathcal{F}_h^{\mathrm{i}}}\mathsf{U}_{\mathcal{F}_h^{\mathrm{i}}}\right)$$

- Face unknowns are obtained solving the global transmission problem

$$\mathsf{A}_h^{\mathrm{sc}}\mathsf{U}_{\mathcal{F}_h^{\mathrm{i}}} = -\mathsf{A}_{\mathcal{T}_h\mathcal{F}_h}^{\mathrm{T}}\mathsf{A}_{\mathcal{T}_h\mathcal{T}_h}^{-1}\mathsf{F}_{\mathcal{T}_h}$$

  with global system matrix

$$\mathsf{A}_h^{\mathrm{sc}} := \mathsf{A}_{\mathcal{F}_h\mathcal{F}_h} - \mathsf{A}_{\mathcal{T}_h\mathcal{F}_h}^{\mathrm{T}}\mathsf{A}_{\mathcal{T}_h\mathcal{T}_h}^{-1}\mathsf{A}_{\mathcal{T}_h\mathcal{F}_h}$$

- $\mathsf{A}_h^{\mathrm{sc}}$ **is SPD and its stencil involves neighbours through faces**

Numerical examples

2d test case, smooth solution, uniform refinement

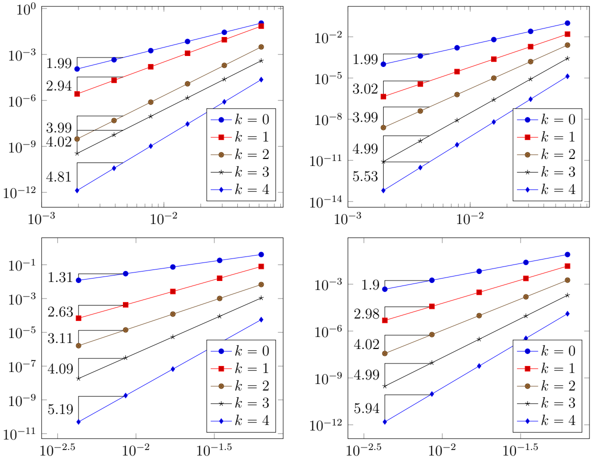

Figure: 2d test case, trigonometric solution. Energy (left) and L^2-norm (right) of the error vs. h for uniformly refined triangular (top) and hexagonal (bottom) mesh families

Numerical examples I

3d industrial test case, adaptive refinement, cost assessment

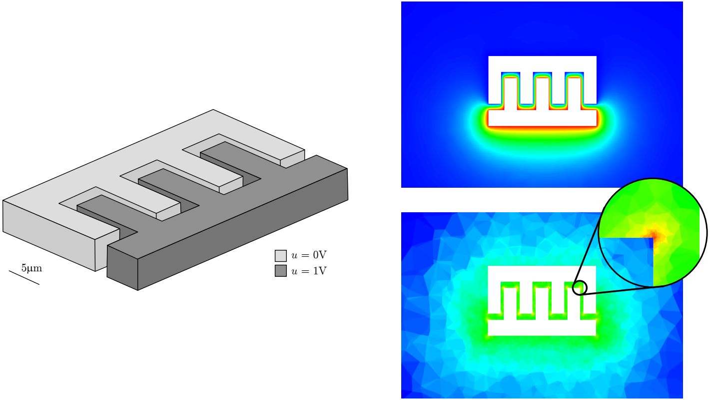

Figure: Geometry (left), numerical solution (right, top) and final adaptive mesh (right, bottom) for the comb-drive actuator test case [DP and Specogna, 2016]

Numerical examples II
3d industrial test case, adaptive refinement, cost assessment

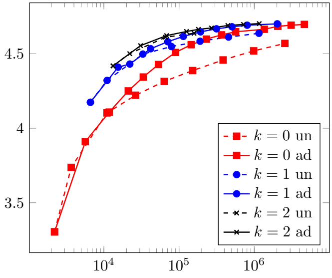

(a) Capacitance vs. $N_{\mathrm{dof},h}$

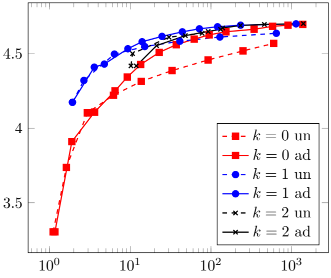

(b) Capacitance vs. computing time

Figure: Results for the comb drive benchmark.

Numerical examples III

3d industrial test case, adaptive refinement, cost assessment

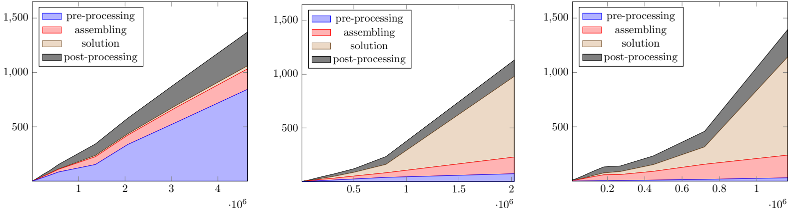

(a) $k = 0$ (b) $k = 1$ (c) $k = 2$

Figure: Computing wall time (s) vs. number of DOFs for the comb drive benchmark, AGMG solver.

Numerical examples I

3d test case, singular solution, adaptive coarsening

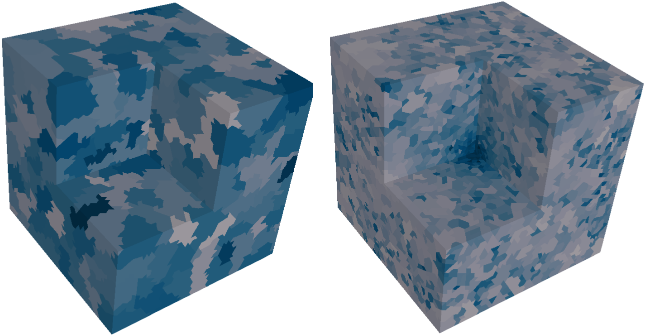

Figure: Fichera corner benchmark, adaptive mesh coarsening [DP and Specogna, 2016]

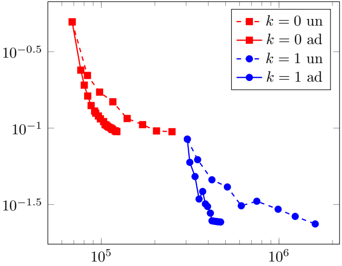

(a) Energy-error vs. N_{dofs}

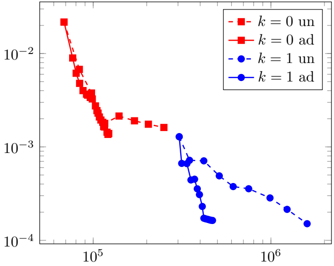

(b) L^2-error vs. N_{ndof}

Figure: Error vs. number of DOFs for the Fichera corner benchmark, adaptively coarsened meshes

Outline

Features

- Construction valid for both $d = 2$ and $d = 3$
- Capability of handling general polyhedral meshes
- Arbitrary approximation order (including $k = 0$)
- Inf-sup stability on general meshes
- Robust handling of dominant advection
- Local conservation of momentum and mass*
- Weakly enforced boundary conditions can be considered*
- Reduced computational cost after static condensation

$$N_{\mathrm{dof},h} = d\,\mathrm{card}(\mathcal{F}_h^{\mathrm{i}})\binom{k-1+d}{d-1} + \binom{k+d}{d}$$

HHO for incompressible flows

- MHO for Stokes [Aghili, Boyaval, DP, 2015]
- Pressure-robust HHO for Stokes [DP, Ern, Linke, Schieweck, 2016]
- Péclet-robust HHO for Oseen [Aghili and DP, 2018]
- Darcy-robust HHO for Brinkman [Botti, DP, Droniou, 2018]
- Skew-symmetric HHO for Navier–Stokes [DP and Krell, 2018]
- Temam's device for HHO [Botti, DP, Droniou, 2018]

The incompressible Navier–Stokes equations I

- Let $d \in \{2, 3\}$, $\nu \in \mathbb{R}_+^*$, $\boldsymbol{f} \in L^2(\Omega)^d$, $\boldsymbol{U} := H_0^1(\Omega)^d$, and $P := L_0^2(\Omega)$
- The INS problem reads: Find $(\boldsymbol{u}, p) \in \boldsymbol{U} \times P$ s.t.

$$\boxed{\begin{aligned} \nu a(\boldsymbol{u}, \boldsymbol{v}) + t(\boldsymbol{u}, \boldsymbol{u}, \boldsymbol{v}) + b(\boldsymbol{v}, p) &= \int_\Omega \boldsymbol{f} \cdot \boldsymbol{v} \qquad && \forall \boldsymbol{v} \in \boldsymbol{U}, \\ -b(\boldsymbol{u}, q) &= 0 && \forall q \in L^2(\Omega), \end{aligned}}$$

with viscous and pressure-velocity coupling bilinear forms

$$a(\boldsymbol{w}, \boldsymbol{v}) := \int_\Omega \boldsymbol{\nabla} \boldsymbol{w} : \boldsymbol{\nabla} \boldsymbol{v}, \quad b(\boldsymbol{v}, q) := -\int_\Omega q \boldsymbol{\nabla} \cdot \boldsymbol{v}$$

and convective trilinear form

$$t(\boldsymbol{w}, \boldsymbol{v}, \boldsymbol{z}) := \int_\Omega (\boldsymbol{w} \cdot \boldsymbol{\nabla}) \boldsymbol{v} \cdot \boldsymbol{z} = \sum_{i=1}^d \sum_{j=1}^d \int_\Omega w_j (\partial_j v_i) z_i$$

Discrete spaces I

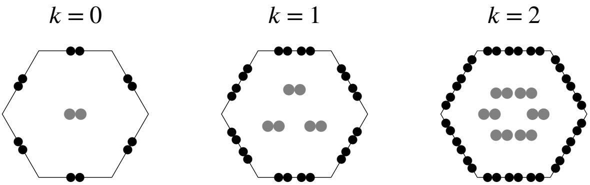

Figure: Local velocity space $\underline{\boldsymbol{U}}_T^k$ for $k \in \{0, 1, 2\}$

- For $k \geq 0$, we define the global space of discrete velocity unknowns

$$\underline{\boldsymbol{U}}_h^k := \Big\{ \underline{\boldsymbol{v}}_h = ((\boldsymbol{v}_T)_{T\in\mathcal{T}_h}, (\boldsymbol{v}_F)_{F\in\mathcal{F}_h}) \ : \\ \boldsymbol{v}_T \in \mathbb{P}^k(T)^d \quad \forall T \in \mathcal{T}_h \text{ and } \boldsymbol{v}_F \in \mathbb{P}^k(F)^d \quad \forall F \in \mathcal{F}_h \Big\}$$

- The restrictions to $T \in \mathcal{T}_h$ are $\underline{\boldsymbol{U}}_T^k$ and $\underline{\boldsymbol{v}}_T = (\boldsymbol{v}_T, (\boldsymbol{v}_F)_{F\in\mathcal{F}_T})$

Discrete spaces II

- The global interpolator $\underline{\boldsymbol{I}}_h^k : H^1(\Omega)^d \to \underline{\boldsymbol{U}}_h^k$ is s.t., $\forall \boldsymbol{v} \in H^1(\Omega)^d$,

$$\underline{\boldsymbol{I}}_h^k \boldsymbol{v} \coloneqq \left((\boldsymbol{\pi}_T^{0,k} \boldsymbol{v}_{|T})_{T \in \mathcal{T}_h}, (\boldsymbol{\pi}_F^{0,k} \boldsymbol{v}_{|F})_{F \in \mathcal{F}_h} \right)$$

- The velocity space strongly accounting for boundary conditions is

$$\underline{\boldsymbol{U}}_{h,0}^k \coloneqq \left\{ \underline{\boldsymbol{v}}_h \in \underline{\boldsymbol{U}}_h^k \ : \ \boldsymbol{v}_F = \boldsymbol{0} \quad \forall F \in \mathcal{F}_h^{\mathrm{b}} \right\}$$

  equipped with the H_0^1-like norm $\|{\cdot}\|_{1,h}$
- The discrete pressure space is defined setting

$$P_h^k \coloneqq \left\{ q_h \in \mathbb{P}^k(\mathcal{T}_h) \ : \ \int_\Omega q_h = 0 \right\} \subset P$$

Gradient, velocity, and divergence reconstructions I

- We define local reconstructions mimicking integration by parts on T
- For $\ell \geq 0$, the gradient reconstruction $\boldsymbol{G}_T^\ell : \underline{\boldsymbol{U}}_T^k \to \mathbb{P}^\ell(T)^{d\times d}$ is s.t.

$$\boxed{\int_T \boldsymbol{G}_T^\ell \underline{\boldsymbol{v}}_T : \boldsymbol{\tau} = -\int_T \boldsymbol{v}_T \cdot (\boldsymbol{\nabla}\cdot\boldsymbol{\tau}) + \sum_{F\in\mathcal{F}_T} \int_F \boldsymbol{v}_F \cdot (\boldsymbol{\tau}\,\boldsymbol{n}_{TF}) \quad \forall \boldsymbol{\tau} \in \mathbb{P}^\ell(T)^{d\times d}}$$

- The velocity reconstruction

$$\boldsymbol{r}_T^{k+1} : \underline{\boldsymbol{U}}_T^k \to \mathbb{P}^{k+1}(T)^d$$

is s.t. $\int_T (\boldsymbol{r}_T^{k+1} \underline{\boldsymbol{v}}_T - \boldsymbol{v}_T) = \boldsymbol{0}$ and

$$\boxed{\int_T (\boldsymbol{\nabla} \boldsymbol{r}_T^{k+1} \underline{\boldsymbol{v}}_T - \boldsymbol{G}_T^k \underline{\boldsymbol{v}}_T) : \boldsymbol{\nabla} \boldsymbol{w} = 0 \quad \forall \boldsymbol{w} \in \mathbb{P}^{k+1}(T)^d}$$

- The divergence reconstruction $D_T^\ell : \underline{\boldsymbol{U}}_T^k \to \mathbb{P}^\ell(T)$ is s.t.

$$\boxed{D_T^\ell \underline{\boldsymbol{v}}_T := \mathrm{tr}(\boldsymbol{G}_T^\ell \underline{\boldsymbol{v}}_T)}$$

Viscous term

- The viscous term is discretized by means of the bilinear form a_h s.t.

$$\mathrm{a}_h(\underline{\boldsymbol{u}}_h, \underline{\boldsymbol{v}}_h) \coloneqq \sum_{T \in \mathcal{T}_h} \mathrm{a}_T(\underline{\boldsymbol{u}}_T, \underline{\boldsymbol{v}}_T)$$

  with local contribution

$$\boxed{\mathrm{a}_T(\underline{\boldsymbol{w}}_T, \underline{\boldsymbol{v}}_T) \coloneqq (\boldsymbol{\nabla} \boldsymbol{r}_T^{k+1} \underline{\boldsymbol{w}}_T, \boldsymbol{\nabla} \boldsymbol{r}_T^{k+1} \underline{\boldsymbol{v}}_T)_T + \mathrm{s}_T(\underline{\boldsymbol{w}}_T, \underline{\boldsymbol{v}}_T)}$$

- As in the scalar case, several possible choices for s_h ensure that

$$\mathrm{a}_h(\underline{\boldsymbol{v}}_h, \underline{\boldsymbol{v}}_h) \simeq \|\underline{\boldsymbol{v}}_h\|_{1,h}^2 \quad \forall \underline{\boldsymbol{v}}_h \in \underline{\boldsymbol{U}}_h^k$$

  with real number C_a independent of h and of the problem data
- Variable viscosity can be treated following [DP and Ern, 2015]

Pressure-velocity coupling

- The pressure-velocity coupling is realized by means of

$$\mathrm{b}_h(\underline{\boldsymbol{v}}_h, q_h) := -\sum_{T \in \mathcal{T}_h} \int_T D_T^k \underline{\boldsymbol{v}}_T q_T$$

- A crucial point is that b_h satisfies the following uniform inf-sup condition: There is $\beta > 0$ independent of h s.t.

$$\boxed{\forall q_h \in P_h^k, \quad \beta \|q_h\|_{L^2(\Omega)} \leq \sup_{\underline{\boldsymbol{v}}_h \in \underline{\boldsymbol{U}}_{h,0}^k, \|\underline{\boldsymbol{v}}_h\|_{1,h}=1} \mathrm{b}_h(\underline{\boldsymbol{v}}_h, q_h)}$$

- This stability result is valid on general meshes and for any $k \geq 0$

A key remark I

- We have the following IBP formula: For all $\boldsymbol{w}, \boldsymbol{v}, \boldsymbol{z} \in H^1(\Omega)^d$,

$$\boxed{\int_\Omega (\boldsymbol{w}\cdot\boldsymbol{\nabla})\boldsymbol{v}\cdot\boldsymbol{z} + \int_\Omega (\boldsymbol{w}\cdot\boldsymbol{\nabla})\boldsymbol{z}\cdot\boldsymbol{v} + \int_\Omega (\boldsymbol{\nabla}\cdot\boldsymbol{w})(\boldsymbol{v}\cdot\boldsymbol{z}) = \int_{\partial\Omega} (\boldsymbol{w}\cdot\boldsymbol{n})(\boldsymbol{v}\cdot\boldsymbol{z})}$$

- Using this formula with $\boldsymbol{w} = \boldsymbol{v} = \boldsymbol{z} = \boldsymbol{u}$, we get

$$t(\boldsymbol{u}, \boldsymbol{u}, \boldsymbol{u}) = \int_\Omega (\boldsymbol{u}\cdot\boldsymbol{\nabla})\boldsymbol{u}\cdot\boldsymbol{u} = -\frac{1}{2}\int_\Omega (\boldsymbol{\nabla}\cdot\boldsymbol{u})(\boldsymbol{u}\cdot\boldsymbol{u}) + \frac{1}{2}\int_{\partial\Omega} (\boldsymbol{u}\cdot\boldsymbol{n})(\boldsymbol{u}\cdot\boldsymbol{u}) = 0,$$

  where we have used the mass equation and the boundary condition
- This shows that the convective term is non-dissipative
- **This is a key property to mimick at the discrete level**

A key remark II

- The discrete velocity may not be divergence-free (and zero on $\partial\Omega$)
- We can used as a starting point modified versions of t:

$$t^{\rm ss}(\boldsymbol{w},\boldsymbol{v},\boldsymbol{z}) \coloneqq \frac{1}{2}\int_\Omega (\boldsymbol{w}\cdot\boldsymbol{\nabla})\boldsymbol{v}\cdot\boldsymbol{z} - \frac{1}{2}\int_\Omega (\boldsymbol{w}\cdot\boldsymbol{\nabla})\boldsymbol{z}\cdot\boldsymbol{v}$$

or, following [Temam, 1979],

$$\boxed{t^{\rm tm}(\boldsymbol{w},\boldsymbol{v},\boldsymbol{z}) \coloneqq \int_\Omega (\boldsymbol{w}\cdot\boldsymbol{\nabla})\boldsymbol{v}\cdot\boldsymbol{z} + \frac{1}{2}\int_\Omega (\boldsymbol{\nabla}\cdot\boldsymbol{w})(\boldsymbol{v}\cdot\boldsymbol{z}) - \frac{1}{2}\int_{\partial\Omega} (\boldsymbol{w}\cdot\boldsymbol{n})(\boldsymbol{v}\cdot\boldsymbol{z})}$$

- For $\star \in \{\rm tm, ss\}$ and all $\boldsymbol{w},\boldsymbol{v} \in H^1(\Omega)^d$,

$$t^\star(\boldsymbol{w},\boldsymbol{v},\boldsymbol{v}) = 0$$

- **Hence $t^\star$ is non-dissipative even if $\boldsymbol{\nabla}\cdot\boldsymbol{w} \neq 0$ and $\boldsymbol{v}_{|\partial\Omega} \neq \mathbf{0}$**

Directional derivative reconstruction

- Let $\underline{\boldsymbol{w}}_T \in \underline{\boldsymbol{U}}_T^k$ represent a velocity field on T
- We let the directional derivative reconstruction

$$G_T^k(\underline{\boldsymbol{w}}_T;\cdot) : \underline{\boldsymbol{U}}_T^k \to \mathbb{P}^k(T)^d$$

is s.t., for all $\boldsymbol{z} \in \mathbb{P}^k(T)^d$,

$$\boxed{\int_T G_T^k(\underline{\boldsymbol{w}}_T;\underline{\boldsymbol{v}}_T)\cdot\boldsymbol{z} = \int_T (\boldsymbol{w}_T\cdot\boldsymbol{\nabla})\boldsymbol{v}_T\cdot\boldsymbol{z} + \sum_{F\in\mathcal{F}_T}\int_F (\boldsymbol{w}_F\cdot\boldsymbol{n}_{TF})(\boldsymbol{v}_F - \boldsymbol{v}_T)\cdot\boldsymbol{z}}$$

- $G_T^k(\underline{\boldsymbol{w}}_T;\underline{\boldsymbol{v}}_T)$ and $\boldsymbol{G}_T^{2k}\underline{\boldsymbol{v}}_T$ are linked: For all $\boldsymbol{z} \in \mathbb{P}^k(T)^d$,

$$\int_T G_T^k(\underline{\boldsymbol{w}}_T;\underline{\boldsymbol{v}}_T)\cdot\boldsymbol{z} = \int_T (\boldsymbol{w}_T\cdot\boldsymbol{G}_T^{2k})\underline{\boldsymbol{v}}_T\cdot\boldsymbol{z} + \sum_{F\in\mathcal{F}_T}\int_F (\boldsymbol{w}_F - \boldsymbol{w}_T)\cdot\boldsymbol{n}_{TF}(\boldsymbol{v}_F - \boldsymbol{v}_T)\cdot\boldsymbol{z}$$

Discrete global integration by parts formula

We mimick at the discrete level the formula:

$$\boxed{\int_\Omega (\boldsymbol{w}\cdot\boldsymbol{\nabla})\boldsymbol{v}\cdot\boldsymbol{z} + \int_\Omega (\boldsymbol{w}\cdot\boldsymbol{\nabla})\boldsymbol{z}\cdot\boldsymbol{v} + \int_\Omega (\boldsymbol{\nabla}\cdot\boldsymbol{w})(\boldsymbol{v}\cdot\boldsymbol{z}) = \int_{\partial\Omega} (\boldsymbol{w}\cdot\boldsymbol{n})(\boldsymbol{v}\cdot\boldsymbol{z})}$$

Proposition (Discrete integration by parts formula)

It holds, for all $\underline{\boldsymbol{w}}_h, \underline{\boldsymbol{v}}_h, \underline{\boldsymbol{z}}_h \in \underline{\boldsymbol{U}}_h^k$,

$$\sum_{T\in\mathcal{T}_h} \int_T \left(G_T^k(\underline{\boldsymbol{w}}_T; \underline{\boldsymbol{v}}_T)\cdot\boldsymbol{z}_T + \boldsymbol{v}_T\cdot G_T^k(\underline{\boldsymbol{w}}_T; \underline{\boldsymbol{z}}_T) + D_T^{2k}\underline{\boldsymbol{w}}_T(\boldsymbol{v}_T\cdot\boldsymbol{z}_T)\right)$$
$$= \sum_{F\in\mathcal{F}_h^{\mathrm{b}}} \int_F (\boldsymbol{w}_F\cdot\boldsymbol{n}_F)\boldsymbol{v}_F\cdot\boldsymbol{z}_F - \sum_{T\in\mathcal{T}_h}\sum_{F\in\mathcal{F}_T} \int_F (\boldsymbol{w}_F\cdot\boldsymbol{n}_{TF})(\boldsymbol{v}_F - \boldsymbol{v}_T)\cdot(\boldsymbol{z}_F - \boldsymbol{z}_T).$$

The term in red reflects the non-conformity of the method.

Convective term I

$$\boxed{t^{\mathrm{tm}}(\boldsymbol{w},\boldsymbol{v},\boldsymbol{z}) \coloneqq \int_\Omega (\boldsymbol{w}\cdot\boldsymbol{\nabla})\boldsymbol{v}\cdot\boldsymbol{z} + \frac{1}{2}\int_\Omega (\boldsymbol{\nabla}\cdot\boldsymbol{w})(\boldsymbol{v}\cdot\boldsymbol{z}) \quad \forall \boldsymbol{w},\boldsymbol{v},\boldsymbol{z}\in\boldsymbol{U}}$$

- Inspired by t^{tm}, we set

$$\mathrm{t}_h(\underline{\boldsymbol{w}}_h,\underline{\boldsymbol{v}}_h,\underline{\boldsymbol{z}}_h) \coloneqq \sum_{T\in\mathcal{T}_h} t_T(\underline{\boldsymbol{w}}_T,\underline{\boldsymbol{v}}_T,\underline{\boldsymbol{z}}_T)$$

where, for all $T\in\mathcal{T}_h$,

$$\boxed{\begin{aligned}\mathrm{t}_T(\underline{\boldsymbol{w}}_T,\underline{\boldsymbol{v}}_T,\underline{\boldsymbol{z}}_T) \coloneqq{}& \int_T G_T^k(\underline{\boldsymbol{w}}_T;\underline{\boldsymbol{v}}_T)\cdot\boldsymbol{z}_T + \frac{1}{2}\int_T D_T^{2k}\underline{\boldsymbol{w}}_T(\boldsymbol{v}_T\cdot\boldsymbol{z}_T)\\ &+ \frac{1}{2}\sum_{F\in\mathcal{F}_T}\int_F (\boldsymbol{w}_F\cdot\boldsymbol{n}_{TF})(\boldsymbol{v}_F-\boldsymbol{v}_T)\cdot(\boldsymbol{z}_F-\boldsymbol{z}_T)\end{aligned}}$$

- The second and third terms embody Temam's device for stability

Discrete problem I

- The discrete problem reads: Find $(\underline{\boldsymbol{u}}_h, p_h) \in \underline{\boldsymbol{U}}_{h,0}^k \times P_h^k$ s.t.

$$\boxed{\begin{aligned} \nu \mathrm{a}_h(\underline{\boldsymbol{u}}_h, \underline{\boldsymbol{v}}_h) + \mathrm{t}_h(\underline{\boldsymbol{u}}_h, \underline{\boldsymbol{u}}_h, \underline{\boldsymbol{v}}_h) + \mathrm{b}_h(\underline{\boldsymbol{v}}_h, p_h) &= \int_\Omega \boldsymbol{f} \cdot \boldsymbol{v}_h \quad && \forall \underline{\boldsymbol{v}}_h \in \underline{\boldsymbol{U}}_{h,0}^k, \\ -\mathrm{b}_h(\underline{\boldsymbol{u}}_h, q_h) &= 0 && \forall q_h \in P_h^k \end{aligned}}$$

- Optionally, upwind stabilisation can be added through the term

$$\mathrm{j}_h(\underline{\boldsymbol{w}}_h; \underline{\boldsymbol{v}}_h, \underline{\boldsymbol{z}}_h) \coloneqq \sum_{T \in \mathcal{T}_h} \sum_{F \in \mathcal{F}_T} \int_F \frac{|\boldsymbol{w}_F \cdot \boldsymbol{n}_{TF}|}{2} (\boldsymbol{v}_F - \boldsymbol{v}_T) \cdot (\boldsymbol{z}_F - \boldsymbol{z}_T)$$

Well-posedness I

Theorem (Existence and a priori bounds)

There exists a solution $(\underline{\boldsymbol{u}}_h, p_h) \in \underline{\boldsymbol{U}}_{h,0}^k \times P_h^k$ *such that*

$$\|\underline{\boldsymbol{u}}_h\|_{1,h} \lesssim \nu^{-1}\|\boldsymbol{f}\|_{L^2(\Omega)^d}, \text{ and } \|p_h\| \lesssim \left(\|\boldsymbol{f}\|_{L^2(\Omega)^d} + \nu^{-2}\|\boldsymbol{f}\|_{L^2(\Omega)^d}^2\right),$$

with hidden constant independent of h *and* ν*.*

Theorem (Uniqueness of the discrete solution)

Assume that the forcing term verifies

$$\|\boldsymbol{f}\|_{L^2(\Omega)^d} \leq C\nu^2$$

with C *hidden constant independent of* h *and* ν *small enough. Then, the solution is unique.*

Convergence I

Theorem (Convergence to minimal regularity solutions)

It holds up to a subsequence, as $h \to 0$,

- $\boldsymbol{u}_h \to \boldsymbol{u}$ *strongly in* $L^p(\Omega)^d$ *for* $\begin{cases} p \in [1, +\infty) & \text{if } d = 2, \\ p \in [1, 6) & \text{if } d = 3; \end{cases}$
- $\boldsymbol{G}_h^k \underline{\boldsymbol{u}}_h \to \boldsymbol{\nabla}\boldsymbol{u}$ *strongly in* $L^2(\Omega)^{d\times d}$*;*
- $\mathrm{s}_h(\underline{\boldsymbol{u}}_h, \underline{\boldsymbol{u}}_h) \to 0$*;*
- $p_h \to p$ *strongly in* $L^2(\Omega)$*.*

If the exact solution is unique, then the whole sequence converges.

Key tools: discrete Sobolev embeddings and Rellick–Kondrachov compactness results from [DP and Droniou, 2017a]

Convergence II

Theorem (Convergence rates for small data)

Assume uniqueness for both $(\underline{\boldsymbol{u}}_h, p_h)$ *and* $(\boldsymbol{u}, p)$. *Assume, moreover, the additional regularity* $(\boldsymbol{u}, p) \in H^{k+2}(\Omega)^d \times H^{k+1}(\Omega)$, *as well as*

$$\|\boldsymbol{f}\|_{L^2(\Omega)^d} \le C\nu^2$$

with C *independent of* h *and* ν *small enough. Then, with hidden constant independent of* h *and* ν,

$$\boxed{\|\underline{\boldsymbol{u}}_h - \underline{\boldsymbol{I}}_h^k \boldsymbol{u}\|_{1,h} + \nu^{-1}\|p_h - \pi_h^{0,k} p\|_{L^2(\Omega)} \lesssim h^{k+1} \mathcal{N}_{\boldsymbol{u},p}.}$$

with $\mathcal{N}_{\boldsymbol{u},p} := (1 + \nu^{-1}\|\boldsymbol{u}\|_{H^2(\Omega)^d})\|\boldsymbol{u}\|_{H^{k+2}(\Omega)^d} + \nu^{-1}\|p\|_{H^{k+1}(\Omega)}$.

Static condensation

- Partition the discrete velocity unknowns as before, and the pressure unknowns into average value + oscillations inside each element
- At each iteration, the linear system has the form

$$\begin{bmatrix} \mathsf{A}_{\mathcal{T}_h\mathcal{T}_h} & \widetilde{\mathsf{B}}_{\mathcal{T}_h} & \mathsf{A}_{\mathcal{T}_h\mathcal{F}_h^{\mathrm{i}}} & \overline{\mathsf{B}}_{\mathcal{T}_h} \\ \mathsf{A}_{\mathcal{F}_h^{\mathrm{i}}\mathcal{T}_h} & \widetilde{\mathsf{B}}_{\mathcal{F}_h^{\mathrm{i}}} & \mathsf{A}_{\mathcal{F}_h^{\mathrm{i}}\mathcal{F}_h^{\mathrm{i}}} & \overline{\mathsf{B}}_{\mathcal{F}_h^{\mathrm{i}}} \\ \widetilde{\mathsf{B}}_{\mathcal{T}_h}^{\mathrm{T}} & 0 & \widetilde{\mathsf{B}}_{\mathcal{F}_h^{\mathrm{i}}}^{\mathrm{T}} & 0 \\ \overline{\mathsf{B}}_{\mathcal{T}_h}^{\mathrm{T}} & 0 & \overline{\mathsf{B}}_{\mathcal{F}_h^{\mathrm{i}}}^{\mathrm{T}} & 0 \end{bmatrix} \begin{bmatrix} \mathsf{U}_{\mathcal{T}_h} \\ \widetilde{\mathsf{P}}_{\mathcal{T}_h} \\ \mathsf{U}_{\mathcal{F}_h^{\mathrm{i}}} \\ \overline{\mathsf{P}}_{\mathcal{T}_h} \end{bmatrix} = \begin{bmatrix} \mathsf{F}_{\mathcal{T}_h} \\ 0 \\ 0 \\ 0 \end{bmatrix}$$

- Static condensation of $\mathsf{U}_{\mathcal{T}_h}$ and $\widetilde{\mathsf{P}}_{\mathcal{T}_h}$ is possible

Flux formulation

Proposition (Flux formulation)

Define the numerical normal traces of the viscous and convective fluxes

$$\Phi_{TF}^{\mathrm{visc}}(\underline{\boldsymbol{u}}_T) := -\nu \boldsymbol{\nabla} \boldsymbol{r}_T^{k+1} \underline{\boldsymbol{u}}_T \boldsymbol{n}_{TF} + \nu \boldsymbol{R}_{TF}^k \underline{\boldsymbol{u}}_T,$$

$$\Phi_{TF}^{\mathrm{conv}}(\underline{\boldsymbol{u}}_T) := \boldsymbol{\pi}_F^k \left[\frac{\boldsymbol{u}_F \cdot \boldsymbol{n}_{TF}}{2} (\boldsymbol{u}_F + \boldsymbol{u}_T) - \frac{|\boldsymbol{u}_F \cdot \boldsymbol{n}_{TF}|}{2} (\boldsymbol{u}_F - \boldsymbol{u}_T) \right],$$

with $\boldsymbol{R}_{TF}^k$ lifting of the viscous stabilisation. Then, for all $T \in \mathcal{T}_h$, we have the following local momentum and mass balances: For any $\boldsymbol{v}_T \in \mathbb{P}^k(T)^d$,

$$\int_T \nu \boldsymbol{\nabla} \boldsymbol{r}_T^{k+1} \underline{\boldsymbol{u}}_T : \boldsymbol{\nabla} \boldsymbol{v}_T - \int_T \boldsymbol{u}_T \cdot (\boldsymbol{u}_T \cdot \boldsymbol{\nabla}) \boldsymbol{v}_T - \frac{1}{2} \int_T D_T^{2k} \underline{\boldsymbol{u}}_T (\boldsymbol{u}_T \cdot \boldsymbol{v}_T)$$
$$- \int_T p_T (\boldsymbol{\nabla} \cdot \boldsymbol{v}_T) + \sum_{F \in \mathcal{F}_T} \int_F \left(\Phi_{TF}^{\mathrm{visc}}(\underline{\boldsymbol{u}}_T) + \Phi_{TF}^{\mathrm{conv}}(\underline{\boldsymbol{u}}_T) + p_T \boldsymbol{n}_{TF} \right) \cdot \boldsymbol{v}_T = \int_T \boldsymbol{f} \cdot \boldsymbol{v}_T$$

and, for all $q_T \in \mathbb{P}^k(T)$,

$$D_T^k \underline{\boldsymbol{u}}_T = 0.$$

Moreover, the numerical normal trace of the global flux is conservative, i.e., for any interface $F \in \mathcal{F}_{T_1} \cap \mathcal{F}_{T_2}$, with $\Phi_{TF}(\underline{\boldsymbol{u}}_T) := \left(\Phi_{TF}^{\mathrm{visc}}(\underline{\boldsymbol{u}}_T) + \Phi_{TF}^{\mathrm{conv}}(\underline{\boldsymbol{u}}_T) + p_T \boldsymbol{n}_{TF} \right)$,

$$\Phi_{T_1 F}(\underline{\boldsymbol{u}}_{T_1}) + \Phi_{T_2 F}(\underline{\boldsymbol{u}}_{T_2}) = \boldsymbol{0}.$$

Convergence rate: Kovasznay flow

- Following [Kovasznay, 1948], let $\Omega := (-0.5, 1.5) \times (0, 2)$ and set

$$\mathrm{Re} := (2\nu)^{-1}, \qquad \lambda := \mathrm{Re} - \left(\mathrm{Re}^2 + 4\pi^2\right)^{\frac{1}{2}}$$

- The components of the velocity are given by

$$u_1(\boldsymbol{x}) := 1 - \exp(\lambda x_1)\cos(2\pi x_2), \qquad u_2(\boldsymbol{x}) := \frac{\lambda}{2\pi}\exp(\lambda x_1)\sin(2\pi x_2),$$

and pressure given by

$$p(\boldsymbol{x}) := -\frac{1}{2}\exp(2\lambda x_1) + \frac{\lambda}{2}\left(\exp(4\lambda) - 1\right)$$

- We monitor the errors

$$\boxed{\underline{\boldsymbol{e}}_h := \underline{\boldsymbol{u}}_h - \underline{\boldsymbol{I}}_h^k \boldsymbol{u}, \qquad \epsilon_h := p_h - \pi_h^{0,k} p}$$

Convergence rate: Kovasznay flow

Strongly enforced BC, upwind stabilisation, $\mathrm{Re} = 40$

N_{dof}	N_{nz}	$\\|\underline{\boldsymbol{e}}_h\\|_{\nu,h}$	EOC	$\\|\boldsymbol{e}_h\\|_{L^2(\Omega)^d}$	EOC	$\\|\epsilon_h\\|_{L^2(\Omega)}$	EOC	τ_{ass}	τ_{sol}
				$k = 0$					
65	736	9.37e-01	–	1.40e-01	–	6.84e-01	–	1.31e-02	8.52e-03
289	3808	1.13e+00	-0.27	5.50e-01	-1.98	1.96e-01	1.80	5.92e-02	4.90e-02
1217	17056	9.14e-01	0.31	2.26e-01	1.28	1.02e-01	0.94	1.02e-01	1.06e-01
4993	71968	6.26e-01	0.55	7.89e-02	1.52	3.52e-02	1.54	3.10e-01	4.46e-01
20225	295456	3.87e-01	0.70	2.47e-02	1.68	9.78e-03	1.85	1.02e+00	2.17e+00
81409	1197088	2.47e-01	0.65	8.06e-03	1.61	3.09e-03	1.66	3.73e+00	1.49e+01
				$k = 1$					
113	2464	7.31e-01	–	5.37e-01	–	2.49e-01	–	2.51e-02	1.72e-02
513	13056	3.83e-01	0.93	1.54e-01	1.80	4.29e-02	2.54	4.77e-02	4.72e-02
2177	59008	1.02e-01	1.90	2.13e-02	2.85	3.98e-03	3.43	1.29e-01	1.79e-01
8961	249984	2.93e-02	1.80	2.97e-03	2.84	6.54e-04	2.61	5.13e-01	1.01e+00
36353	1028224	8.23e-03	1.83	3.99e-04	2.90	1.28e-04	2.35	2.05e+00	5.28e+00
146433	4169856	2.26e-03	1.86	5.21e-05	2.94	2.65e-05	2.27	7.25e+00	2.97e+01
				$k = 2$					
161	5216	3.50e-01	–	2.09e-01	–	6.42e-02	–	3.44e-02	2.26e-02
737	27872	3.76e-02	3.22	1.34e-02	3.96	2.07e-03	4.95	6.95e-02	6.88e-02
3137	126368	6.96e-03	2.43	1.31e-03	3.36	1.48e-04	3.80	2.66e-01	3.60e-01
12929	536096	1.06e-03	2.72	9.48e-05	3.79	1.77e-05	3.07	1.11e+00	2.02e+00
52481	2206496	1.55e-04	2.77	6.36e-06	3.90	2.27e-06	2.96	4.16e+00	1.13e+01
211457	8951072	2.21e-05	2.81	4.13e-07	3.95	2.72e-07	3.06	1.51e+01	6.02e+01
				$k = 5$					
305	19616	2.28e-03	–	1.05e-03	–	1.70e-04	–	1.28e-01	5.63e-02
1409	105728	4.01e-05	5.83	1.05e-05	6.65	2.05e-06	6.37	3.95e-01	2.19e-01
6017	480896	7.21e-07	5.80	8.98e-08	6.87	3.21e-08	6.00	1.60e+00	1.32e+00
24833	2043008	1.37e-08	5.72	7.89e-10	6.83	5.43e-10	5.88	6.45e+00	8.29e+00
100865	8414336	2.56e-10	5.74	6.72e-12	6.88	9.14e-12	5.89	2.54e+01	5.01e+01

Convergence rate: Kovasznay flow

Weakly enforced BC, no stabilisation, $\mathrm{Re} = 40$

N_{dof}	N_{nz}	$\|\underline{\boldsymbol{e}}_h\|_{\nu,h}$	EOC	$\|\boldsymbol{e}_h\|_{L^2(\Omega)^d}$	EOC	$\|\epsilon_h\|_{L^2(\Omega)}$	EOC	τ_{ass}	τ_{sol}
				$k=0$					
97	1216	1.07e+00	–	3.93e-01	–	6.80e-01	–	2.68e-02	2.31e-02
353	4800	1.70e+00	-0.67	9.58e-01	-1.28	2.79e-01	1.28	3.41e-02	3.71e-02
1345	19072	1.44e+00	0.24	3.89e-01	1.30	1.32e-01	1.09	6.68e-02	8.04e-02
5249	76032	8.77e-01	0.72	1.18e-01	1.72	4.93e-02	1.42	2.15e-01	3.52e-01
20737	303616	4.78e-01	0.88	3.23e-02	1.87	1.49e-02	1.72	8.07e-01	1.95e+00
82433	1213440	2.46e-01	0.96	8.32e-03	1.96	4.08e-03	1.87	3.19e+00	1.47e+01
				$k=1$					
177	4256	1.02e+00	–	7.27e-01	–	2.69e-01	–	1.44e-02	1.60e-02
641	16768	4.20e-01	1.28	1.66e-01	2.13	4.96e-02	2.44	3.59e-02	4.25e-02
2433	66560	1.40e-01	1.58	2.66e-02	2.64	8.60e-03	2.53	1.09e-01	1.70e-01
9473	265216	4.06e-02	1.79	3.55e-03	2.91	1.29e-03	2.74	4.62e-01	1.10e+00
37377	1058816	1.03e-02	1.97	4.37e-04	3.02	1.79e-04	2.85	1.91e+00	5.64e+00
148481	4231168	2.61e-03	1.99	5.46e-05	3.00	2.96e-05	2.60	7.07e+00	3.32e+01
				$k=2$					
257	9152	5.50e-01	–	3.16e-01	–	1.20e-01	–	2.23e-02	2.33e-02
929	36032	7.58e-02	2.86	2.46e-02	3.68	6.03e-03	4.31	6.11e-02	7.47e-02
3521	142976	1.23e-02	2.62	1.84e-03	3.74	3.69e-04	4.03	2.41e-01	3.90e-01
13697	569600	1.70e-03	2.86	1.12e-04	4.03	3.63e-05	3.35	1.02e+00	2.21e+00
54017	2273792	2.21e-04	2.95	6.87e-06	4.03	3.84e-06	3.24	3.62e+00	1.17e+01
214529	9085952	2.80e-05	2.98	4.28e-07	4.00	3.72e-07	3.37	1.40e+01	6.76e+01
				$k=5$					
497	34976	6.48e-03	–	1.76e-03	–	1.02e-03	–	1.23e-01	7.22e-02
1793	137600	7.07e-05	6.52	1.34e-05	7.04	4.58e-06	7.81	4.06e-01	2.95e-01
6785	545792	1.28e-06	5.79	1.10e-07	6.94	4.40e-08	6.70	1.51e+00	1.56e+00
26369	2173952	2.20e-08	5.87	8.84e-10	6.95	5.86e-10	6.23	5.67e+00	8.48e+00
103937	8677376	3.56e-10	5.95	7.20e-12	6.94	7.42e-12	6.30	2.28e+01	5.14e+01

Lid-driven cavity I

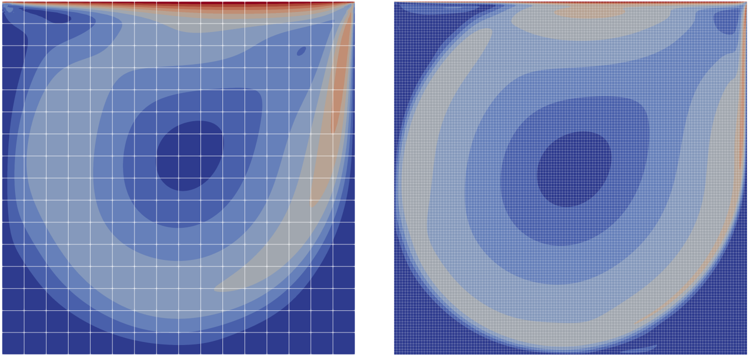

Figure: Lid-driven cavity, velocity magnitude contours (10 equispaced values in the range $[0, 1]$) for $k = 7$ computations at $\mathrm{Re} = 1{,}000$ (*left*: 16x16 grid) and $\mathrm{Re} = 20{,}000$ (*right*: 128x128 grid).

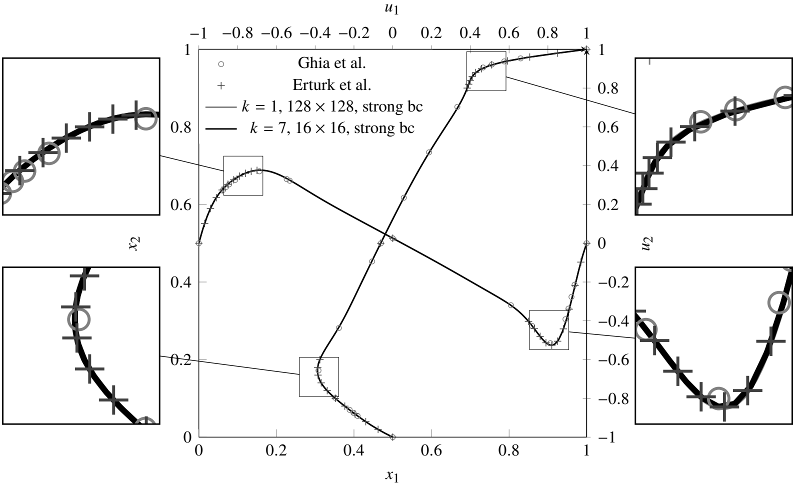

Figure: u_1 along the vertical centerline, u_2 along the horizontal centerline

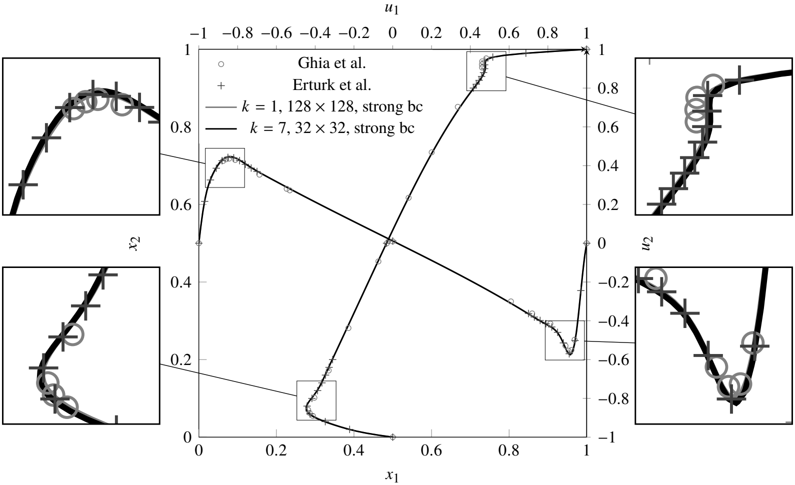

Figure: u_1 along the vertical centerline, u_2 along the horizontal centerline

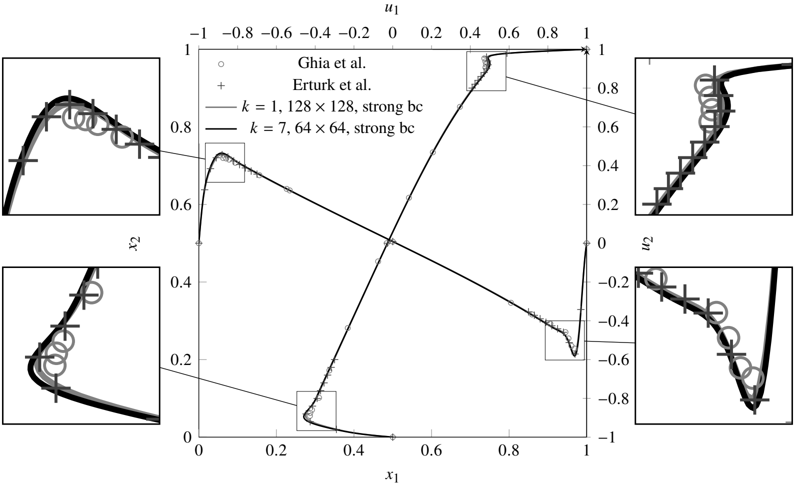

Figure: u_1 along the vertical centerline, u_2 along the horizontal centerline

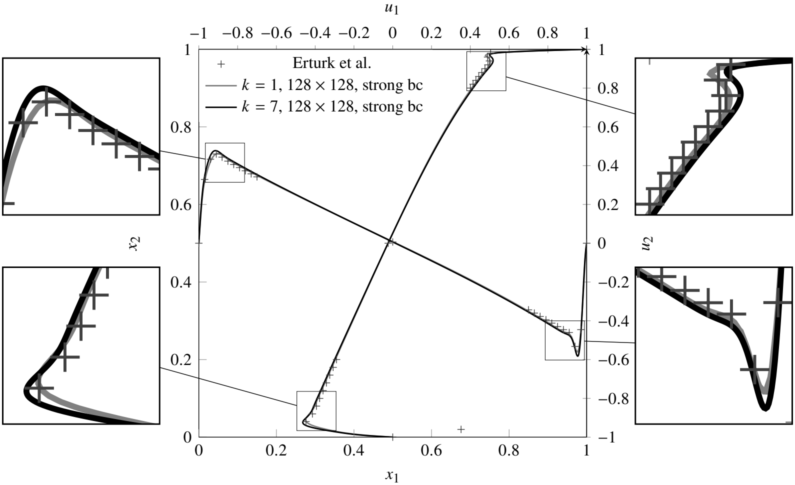

Figure: u_1 along the vertical centerline, u_2 along the horizontal centerline

References I

Aghili, J., Boyaval, S., and Di Pietro, D. A. (2015).
Hybridization of mixed high-order methods on general meshes and application to the Stokes equations.
Comput. Meth. Appl. Math., 15(2):111–134.

Aghili, J. and Di Pietro, D. A. (2018).
An advection-robust Hybrid High-Order method for the Oseen problem.
J. Sci. Comput.
Published online.

Botti, L., Di Pietro, D. A., and Droniou, J. (2018a).
A Hybrid High-Order discretisation of the Brinkman problem robust in the Darcy and Stokes limits.
Comput. Methods Appl. Mech. Engrg.
Accepted for publication.

Botti, L., Di Pietro, D. A., and Droniou, J. (2018b).
A Hybrid High-Order method for the incompressible Navier–Stokes problem based on Temam's device.
Submitted.

Di Pietro, D. A. and Droniou, J. (2017a).
A Hybrid High-Order method for Leray–Lions elliptic equations on general meshes.
Math. Comp., 86(307):2159–2191.

Di Pietro, D. A. and Droniou, J. (2017b).
$W^{s,p}$-approximation properties of elliptic projectors on polynomial spaces, with application to the error analysis of a Hybrid High-Order discretisation of Leray–Lions problems.
Math. Models Methods Appl. Sci., 27(5):879–908.

Di Pietro, D. A. and Droniou, J. (2018).
A third Strang lemma for schemes in fully discrete formulation.
Submitted.

References II

Di Pietro, D. A. and Ern, A. (2015).
A hybrid high-order locking-free method for linear elasticity on general meshes.
Comput. Methods Appl. Mech. Engrg., 283:1–21.

Di Pietro, D. A., Ern, A., Linke, A., and Schieweck, F. (2016).
A discontinuous skeletal method for the viscosity-dependent Stokes problem.
Comput. Meth. Appl. Mech. Engrg., 306:175–195.

Di Pietro, D. A. and Krell, S. (2018).
A Hybrid High-Order method for the steady incompressible Navier–Stokes problem.
J. Sci. Comput., 74(3):1677–1705.

Di Pietro, D. A. and Specogna, R. (2016).
An a posteriori-driven adaptive Mixed High-Order method with application to electrostatics.
J. Comput. Phys., 326(1):35–55.

Di Pietro, D. A. and Tittarelli, R. (2018).
Numerical Methods for PDEs – State-of-the-art Numerical Techniques, chapter An introduction to Hybrid High-Order methods.
Springer.
No 15 in SEMA-SIMAI Series.

Kovasznay, L. S. G. (1948).
Laminar flow behind a two-dimensional grid.
Proc. Camb. Philos. Soc., 44:58–62.

Temam, R. (1979).
Navier-Stokes equations, volume 2 of *Studies in Mathematics and its Applications*.
North-Holland Publishing Co., Amsterdam-New York, revised edition.
Theory and numerical analysis, With an appendix by F. Thomasset.